AIMS Materials Science, 8(4): 587–607.
DOI: 10.3934/matersci.2021036
Received: 01 April 2021
Accepted: 23 June 2021
Published: 16 July 2021

http://www.aimspress.com/journal/Materials

Research article

Numerical and experimental investigation of concrete with various dosages of fly ash

Kong Fah Tee* and Sayedali Mostofizadeh

School of Engineering, University of Greenwich, Kent ME4 4TB, UK

* **Correspondence:** Email: K.F.Tee@gre.ac.uk; Tel: +44(0)1634883141.

Abstract: The nonlinear behavior of reinforced fly ash concrete (RFAC) beams until the ultimate failure is highly a multifaceted phenomenon due to the contention of heterogeneous material properties and the cracking behavior of concrete. This paper represents an exploration of nonlinear finite element analysis of reinforced concrete beams with the inclusion of fly ash under flexural loading. Finite element modelling of RFAC beams is carried out using a distinct reinforcement modelling method. The capability of the model to capture the critical crack regions, loads and deflections for various loadings in RFAC beams has been evaluated. Comparison is made between experimental results and finite element modelling with respect to crack formation and the ultimate capacity for flexural loading and mid-span deflection. The achieved results in the present study indicate acceptable approximation with those in the previous investigations.

Keywords: fly ash; concrete cube; concrete beam; reinforced concrete; finite element modelling

1. Introduction

In recent decades, the improvement in the construction industry has contributed extremely due to new developments in the usage of pozzolanic materials [1–2]. Fly ash (FA) as the artificial pozzolan in a concrete mixture is capable to alert the properties of strength, durability, and ductility in the reinforced concrete (RC) structures [3–5]. Indeed, RC has become the most significant building material which is widely used in many engineering structures. Some unique properties such as economy, efficiency, high strength, and stiffness have made the RC an attractive material for a wide range of structural usages. Therefore, recognizing the appropriate response of structural elements and the nonlinear behavior of concrete are two main points for the improvement of the

overall efficiency and safety of the structure. Hence, the performance of RC beams is to be investigated through full-scale laboratory tests. Also, the experimental observations are compared to theoretical calculations that estimate deflections and ultimate forces within the beam. Finite Element Modelling (FEM) can also be employed to model the behavior of structure numerically to obtain these calculations which are in good agreement with laboratory investigations, especially in parametric studies [6–7].

In the case of the role of low calcium-FA (LCFA) on the development of concrete properties, a series of studies were conducted to experimentally evaluate the mechanical and physical properties of concrete containing a variety of FA dosages. Golewski [8] investigated the impact of ambient curing conditions on the fracture toughness of concrete with the inclusion of 20% and 30% LCFA. The laboratory results demonstrated that the highest increase in fracture toughness, as one of the mechanical properties of concrete, was observed over the initial 28 d. Also, the concrete specimens involving LCFA were mainly characterized through a quasi-plastic process of failure compared to those without LCFA additives [8]. Golewski [9] has also driven the further improvement of fracture toughness through participating in other pozzolanic materials such as silica fume (SF) in nanoscale for concrete mixtures. Based on the experimental results, the optimal concrete mix design for fracture toughness belongs to those concrete specimens involving the proportion of 10% FA + 10% SF as the replacement of cement in the first 28 d [9]. On the other hand, the beneficial aspect of FA in concrete content for reducing the size of microcracks in the interfacial transition zone under dynamic loading (ITZ) has also been explored in another investigation by Godlewski [10]. The results reveal that the utilization of 20% FA additive has a considerable effect on the reduction of average width microcracks (W_C), whereas the average value of Wc in the case of concrete mixes containing 30% FA had greater microcracks in ITZ than that of mixtures without FA [10].

As for other mechanical properties of concrete, Lisantono et al. [11] studied the flexural behavior of RFAC beams experimentally by using two beams as control beams and six other beams with high-value fly ash concrete as the replacement of Portland cement (PC) by weighing with dosages of 50%, 60% and 70%. Annapurna et al. [12] introduced the route to develop FA based geopolymer concrete (GPC) for RC beams. They described the experimental program and the numerical work using FEM. The study showed that the use of FEM through ANSYS to model experimental data was viable and the results were reasonably close. Karnati [13] used an RC beam in a rectangular shape having a length of 2400 mm, a width of 150 mm, and a depth of 250 mm which was reinforced with two different types of main bars. In this research, the validated RC beam was investigated for flexural strength of concrete beams containing 25% of FA using FEM by utilizing ANSYS. The results of FEM demonstrated that the structural response of RC beams is exclusively associated with mechanical properties which are in relation to compressive strength concrete (fc) and is particularly sensitive to elasticity modulus (Ec). Dahmeni et al. [14] investigated crack propagation in RC beams using ANSYS and modelled with solid 65 elements with smeared reinforcement approach. Also, Vasudevan and Khothandaraman (2012) carried out a nonlinear analysis of six RC beams by ANSYS in accordance with IS 456:2000 guidelines and the numerical results were accurately compared with analytical calculations [15].

The novelty of this study, as the significant motivation, is to assess the concurrent effects of concrete properties and ambient conditions in experimental tests such as heat, alkaline solution on the improvement of flexural strength in RFAC beams with the inclusion of various dosages through conducting numerical simulations with utilizing the obtained data from laboratory programs.

Therefore, the first stage is to identify the significant factors in nonlinear analysis such as time steps, optimal mesh size, and effective concrete properties such as elasticity modulus, open and closed shear coefficients in the developed FE software utilizing solid 65 elements as smeared crack model considered for RFAC beams. Also, the flexural strength of the RFAC beam has accurately been investigated for all dosages of FA (0–70%) by assessing the optimal response of RFAC beams while gradually enhancing the dosage of FA along with the effectiveness of other laboratory ambient conditions in the numerical simulation carried out for the first time in this study. Certainly, the accuracy of the flexural response of concrete, with the consideration of all experimental and numerical parameters, can be seen as the key motivation for improving the serviceability performance of RFAC beams. Typically, serviceability is directly in relation to the enhancement of compressive and flexural strength of concrete. On the other hand, the usage of FA with optimal dosage in RFAC beams can be considered as a beneficial mixture providing high durability and serviceability as well as adequate strength. In addition, it plays a significant role in eco-friendly fields. This means that the use of FA in RFAC beams leads to the lower consumption of PC emitting the largest amount of CO_2 in the atmosphere. FA also reduces the construction costs of concrete structures due to cheaper and more abundant than PC.

As discussed above, the non-linear behavior of materials in concrete models containing various percentages of FA with the use of commercially available finite element (FE) software ANSYS v 18.2 is numerically investigated. The initial aim of this study is to evaluate ultimate load, mid-span load-displacement relationship, and crack developments in RC beams for these concrete types. The novelty of this study is the concurrent evaluation of the effects of concrete properties with experimental factors such as heat, alkaline solution (AS), and numerical analysis on the development of flexural strength in RFAC beams with the inclusion of various dosages of FA. The validation of the model is simulated based on the experimental and numerical results achieved from the previous studies. In the first attempt, the beam model used by Karnati [13] is considered in the first numerical example for calibration of RC with the inclusion of 25% of FA. This research also compares the results of the flexural response of RC beams with dosages of 0%, 50%, 70% of FA obtained from the experimental program conducted by Lisantono et al. [11] through calibrating in ANSYS software. Next, experimental and numerical investigation indicates the flexural response of RC beams with different values of FA (0%, 10%, 20%, 30%, 50%, 70%) as the replacement of Type 2 Portland cement (T2PC), in which the compressive strength of concrete at 28 d and other mechanical properties are experimentally achieved in the laboratory under different curing conditions.

2. Materials constitutive model in FEM

The linear and non-linear isotropic concrete material properties are used to properly model RC beams in this study. According to the analysis type, material properties in linear and nonlinear phases have been defined in ANSYS [16]. The Young's modulus is considered from the empirical expression recommended by Hardjito which has the relatively high approximation to the values of elasticity modulus measured in the experimental study carried out by Nguyen et al. [17] on mechanical properties of GPC concrete. Thus, Eq 1 is used in this study.

$$Ec = 2707\sqrt{f_{cm}} + 5300\ (MPa) \tag{1}$$

where f_{cm} is the mean compressive strength (MPa).

The modified Popovic's stress-strain model is proposed for the stress-strain curve of experimental specimens in this research which is similar to that for normal strength concrete. However, to achieve the strain subjected to the degraded strength, an iterative method is needed such as the Newton–Raphson method [18,19] as shown in Eq 2.

$$fc2 = fp.\frac{n\left(\frac{\varepsilon c2}{\varepsilon p}\right)}{(n-1)+(\varepsilon c2/\varepsilon p)^{nk}} \quad (2)$$

where *n* can be calculated as shown below:

$k = 0.6 - \frac{fp}{62}$ for $\varepsilon c2 < \varepsilon p < 0, n = 0.80 - fp/17$, $\varepsilon p = \frac{fp}{Ec}\left(\frac{n}{n-1}\right)$.

where *n* is a curve-fitting parameter for the stress-strain response of concrete in compression; *k* is a post decay parameter for the stress-strain response of concrete in compression and *fp* is peak concrete compressive stress. $f'c$ is used as peak compressive strength rather than *fp* in this research. In ANSYS software, Von Mises and William-Warenke failure criteria are employed for steel and concrete materials, respectively. In the case of the materials such as rock and soil, the Dracker–Prager criterion is chosen. In ANSYS APDL, the "Concrete" model is used to simulate the nonlinear behavior of concrete, which is approximately derived from the William-Warenke failure criterion. This model is capable of evaluating both concrete damages due to cracking in the tension region and crushing in the compression region [20,21]. Thus, the William-Warenke failure criterion has been used for predicting the nonlinear behavior of concrete.

To define the material in this model, 9 parameters are required as follows:

(1) The shear transfer coefficient for open cracks *βt*
(2) The shear transfer coefficient for closed cracks *βc*
(3) Uniaxial cracking stress *fr*
(4) Uniaxial crushing stress $f'c$
(5) Biaxial crushing stress $f'cb$
(6) Hydrostatic pressure (Tri-axial) σh
(7) Hydrostatic biaxial crush stress *f1*
(8) Hydrostatic uniaxial crush stress *f2*
(9) Tensile crack factor

The range of typical shear transfer coefficients is from 0 to 1, representing a smooth crack and 1 representing a rough crack. The shear transfer for open and closed cracks are determined based on the study carried out by Kachlakev et al. [22] as a basis. The problems associated with convergence can occur when the shear transfer coefficient for open crack drops below 0.2. Thus, the open crack is considered as the lowest possible value which is 0.2. The shear coefficient for closed crack is typically in the range of 2–4 times of open crack value (βc = 2–4 βt) following previous investigations in this field. The uniaxial cracking stress is determined using fr =7.5$\sqrt{f'c}$ [21,23].

The convergence issues have commonly been reported when the crushing capability is turned on. The biaxial crushing stress refers to the ultimate biaxial compressive strength ($f'cb$). The ambient hydrostatic stress state is denoted as σh. This stress state is defined in Eq 3:

$$\sigma h = \frac{1}{3}(\sigma xp + \sigma yp + \sigma zp) \quad (3)$$

where $\sigma xp, \sigma yp$, and σzp are the principal stresses in principal directions. The biaxial crushing stress under the ambient hydrostatic stress state refers to the ultimate compressive strength for a state of biaxial compression superimposed on the hydrostatic stress state ($f1$). The uniaxial crushing stress under the ambient hydrostatic stress state refers to the ultimate compressive strength for a state of uniaxial compression superimposed on the hydrostatic stress state ($f2$). In concrete, tensile failure occurs when the tensile stress in the principal direction exceeds the tensile strength (ft) [20]. Thus, the failure surface can be defined with the minimum of two constants, ft and $f'c$. The remainder of the variables in the concrete model is left to default based on Eqs 4–6 [21]:

$$f'cb = 1.2f'c \tag{4}$$

$$f'1 = 1.4f'c \tag{5}$$

$$f'2 = 1.75f'c \tag{6}$$

These stress states are only valid for satisfying the condition in Eq 7.

$$\sigma h \leq \sqrt{3}\, f'c \tag{7}$$

3. FEM or RC beams using ANSYS

3.1. Modelling and Meshing

In this study, the beam is modelled by creating the volumes based on the desired dimensions for each stage. The solid 65 elements are typically used for concrete material in ANSYS [16]. To achieve the proper results from solid 65 elements, a rectangular mesh is used. The elements of reinforcement are created in the modelling through the created nodes by the mesh of concrete volume. Therefore, it is important to use the command of "merge items" to assemble separate entities which have the same location. Also, the boundary conditions are essential to constrain the model to obtain a unique solution. This step is necessary to ensure that the performance of the model is the same way as the experimental beam, boundary conditions need to be applied at the supports and loading. Therefore, the support is to model in such a way that a roller and hinge is created. The force is applied as a distributed load on the nodes of the steel plate which are on the top surface of concrete beams. The solid 188 is chosen for two steel plates in this study.

3.2. Nonlinear analysis

In nonlinear analysis, the total load used for FEM is divided into a number of load increment under time steps with different sizes which are called load steps. The stiffness matrix of the model is adjusted to reflect nonlinear change before proceeding to the next load enhancement after completing each incremental solution. Newton–Raphson equilibrium iteration is used for ANSYS software to update the model stiffness. Indeed, Newton–Raphson equilibrium iterations can provide convergence at the end of each load increment within tolerance limits [24].

3.3. Load stepping and failure description for FEM

In the case of nonlinear analysis, automatic time stepping (ATS) in the ANSYS has the capability to predict and control load step sizes. Hence, ATS can increase the load increment up to the highest load step size provided that the convergence behavior is smooth. This can be happened based on the previous solution history and the physical properties of the model. The maximum and minimum load step size are the main inputs for ATS. So, the failure of the models can occur at the time when the solution for the defined load increment still does not converge. Consequently, the program gives the error message showing that the model has a significantly large deflection beyond the displacement limitations considered in the ANSYS.

4. Numerical Calibration with Karnati [13] (Case 1)

4.1. Problem statement

In the first stage, for the calibration of modelling and recognizing analysis technique, the concrete models used by Karnati [13] are numerically investigated. Karnati validated the experimental beam tests obtained by Chahrour and Soudki [25] with finite element modelling (FEM). This calibration demonstrated that the obtained results from FEM were in close agreement with experimental results of 0% FA. Subsequently, various substitutes of concrete were numerically simulated through FEM utilizing ANSYS 18.2 in this paper. So, the properties of the RFAC beam containing 25% FA, in which the mechanical properties of this concrete type were experimentally obtained by Ramazanianpour et al. [26], were numerically calibrated with the RC beam.

In this stage, the FEM used in the study is validated through employing ANSYS 18.2 with the use of details given by Karnati [13]. The mechanical properties of concrete are presented in Table 1. The FEM of the beam is shown in Figure 1. The left and right supports are modelled as hinged and roller, respectively by constraining the displacement in the relevant directions.

Table 1. Property of steel and concrete for RC beam with 25% FA.

Property	Value
Compressive strength at 28 d age (MPa)	31.6
Modulus of elasticity for concrete (MPa)	26000
Yield strength of steel bar (MPa)	400000
Poisson ratio for steel	0.3
Poisson ratio for concrete	0.25
β (t)	0.15
Modulus of rapture (Fr) MPa	3.92

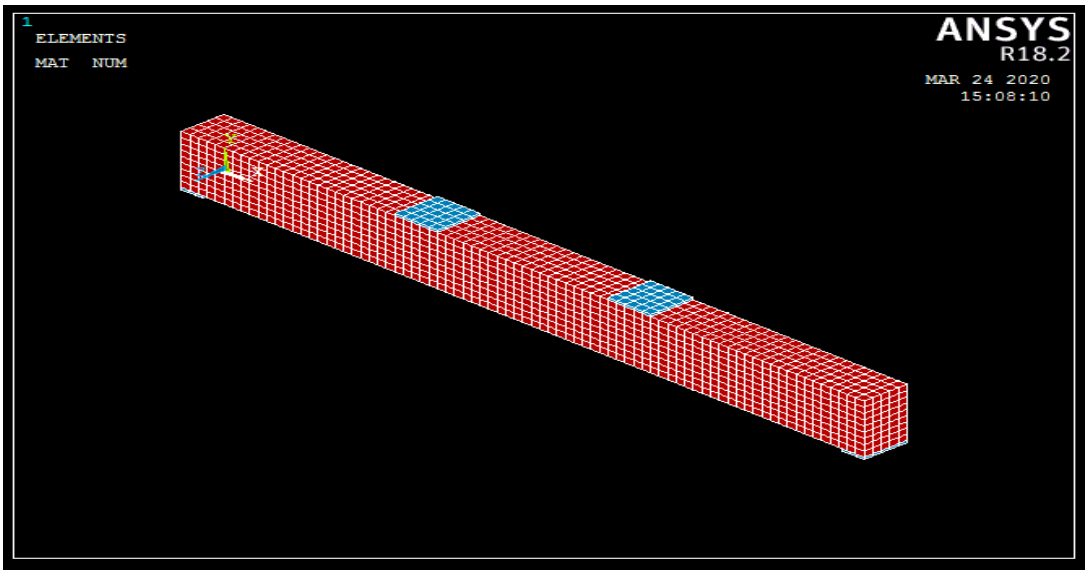

Figure 1. FEM of the beam for numerical simulation.

4.2. Results and discussion

According to Figure 2, the plot of load vs mid-span deflection in the present study clearly indicates the comparison of load and center-line deflection at the failure of the concrete beam. The obtained results are compared to those previously reported by Karnati [13] in this study. The behavior of load-deflection and centerline deflection in FEM is accurately compared to numerical data achieved from the RC beam as the control concrete beam with 0% FA. The mode of failure for the RC beam is modelled quite well employing FEM which shows that the prediction of failure load is quite close to the failure load experimentally measured during laboratory tests (Table 2). Also, bi-linear behavior in terms of load vs. mid-span deflection curve is observed which is approximately matching with the available results in the literature.

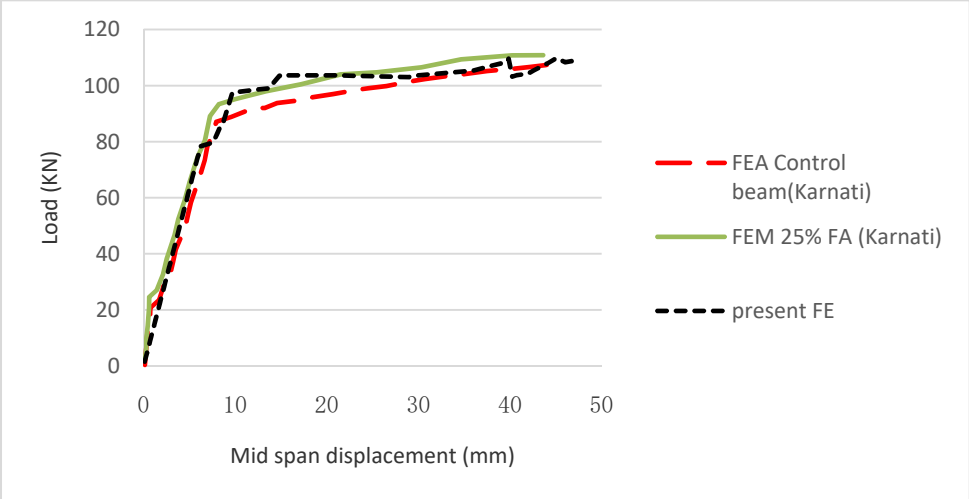

Figure 2. Load-displacement curve for numerical simulation (Case 1).

Table 2. Comparison of the results of flexural analysis for numerical simulation (Case 1).

Beam	First cracking load (kN)	Ultimate load (kN)	Mid-span deflection (mm)
FE present study for 25% FA	18.73	108.93	47.03
FE study for 0% FA [22]	21.87	108.03	45.09
FE study for 25% FA [10]	18.14	110.83	43.61

5. Numerical Calibration with Lisantono et al. [8] (Case 2)

5.1. Problem Statement

The concrete beam models experimentally investigated by Lisantono et al. [11] is considered in this section of the study. The three-dimensional nonlinear FEM of an RC beam has been explored by Lisantono et al. [11] as well. Two RC beams are used as control beams without using FA, whereas four others RFAC beams are used with high-volume FA concrete containing 50% and 70% of FA as the replacement of Portland cement by mass. Six RC beam specimens were examined in this study based on the laboratory standards used for structures and materials. Thus, the actuator with a load capacity of 250 kN was considered for all RC beams. The dimensions of RC beams are 2300 mm × 260 mm × 150 mm which are approximately similar to those of the study carried out by Karnati [13]. A two-point loading system is simply supported and symmetrically loaded in this study which is the same as used in the previous simulation in section Numerical Calibration with Karnati [13] (Case 1). Solid 65 is used for concrete to better simulate the different types of concrete element as some distinct properties such as crashing strength in compression and cracking in tension are considered by smeared crack approach. Smeared reinforcement method was developed by Dahmani et al. [14]. In the present study, concrete reinforcement was defined as the percentage of steel amounts embedded in concrete for numerical simulations.

The potency of FEM to recognize the critical crack region and loads as well as deflections for various types of loading in RC beams has been illustrated. In the present study, the validation is conducted based on the same geometry, sizes and material properties with discrete reinforcement modelling and numerical results are compared with that of literature.

5.2. Results and discussion

Load-displacement curves are presented in Figure 3. The close approximation with the available literature [11] can be seen in the elastic and nonlinear zone. The first cracks of the RC and RFAC specimens experimentally obtained in the study by Lisantono et al. [11] have close accuracy with those of the present study virtually investigated through ANSYS (Table 3). Therefore, it can be seen that the average first crack load of RFAC beams decreases while the value of FA as the substitution of PC is enhanced. Also, the value of the ultimate load for each RC beam specimen is presented in Table 4. It can be noted that the average ultimate load of the RFAC beam containing a high dosage of FA is lower than that of the RC beam as concrete control beam for both the experimental program and numerical results of the present study. The RFAC beam with 50% FA is the optimum replacement of PC as it has a higher value of ultimate load compared to the RFAC beam with 70% FA. Thus, this demonstrates that the RFAC beam with 50% FA has higher shear strength than that with 70% FA.

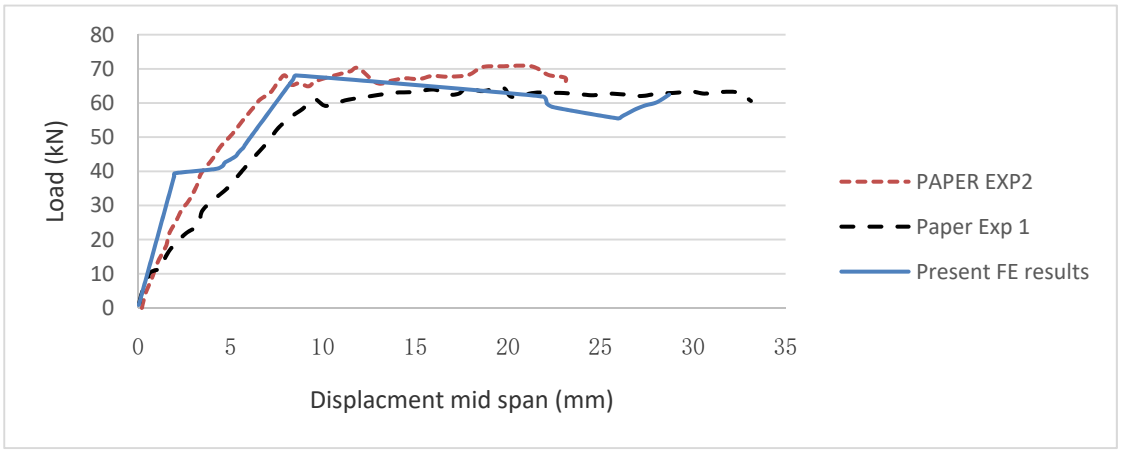

(a)

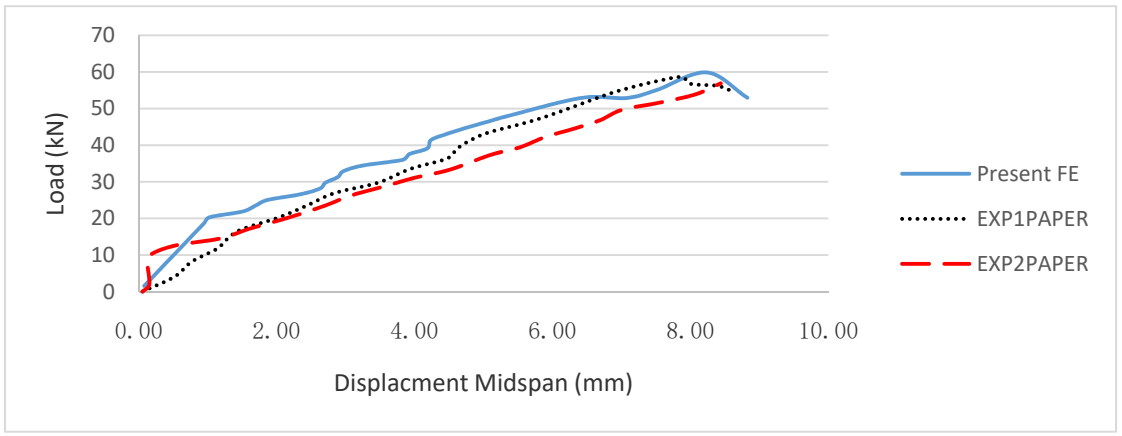

(b)

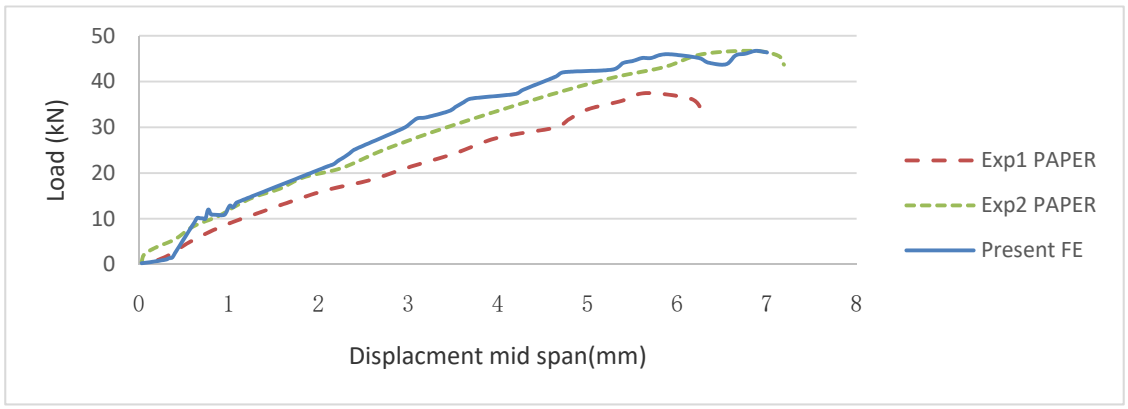

(c)

Figure 3. Load-displacement curve for RC beams with (a) 0% FA, (b) 50% FA, (c) 70% FA.

Table 3. The first cracking load of every beam specimen for numerical simulation (Case 2).

FA content	The load at first crack (kN) (Experimental test by [8])	Average load at first crack (kN) [8]	The load at first crack (kN) (FE Present study)
0%	26.12	31.31	35.12
0%	36.50		
50%	25.50	22.30	26.24
50%	19.10		
70%	21.85	18.55	22.54
70%	15.25		

Table 4. The ultimate load of beam specimens for numerical simulation (Case 2).

Beam designation	FA content	Average ultimate load (kN) (Experimental test by [8])	Average ultimate load (kN) (Present FEM)
Control RC beam	0	70.003	68.09
RFAC beam EXP test 1	50	57.263	59.87
RFAC beam EXP test 2	70	41.893	46.7

6. Numerical and experimental investigation (Case 3)

6.1. Results and discussion

Having obtained the calibration of experimental and numerical results with acceptable accuracy in sections Numerical Calibration with Karnati [13] (Case 1) and Numerical Calibration with Lisantono et al. [8] (Case 2), the flexural strength of RFAC beams containing FA with the values of 10, 20, 30, 50 and 70% as the replacement of T2PC is investigated in the present investigation. The main aim of this research is to assess the concurrent effects of FA, curing conditions and alkaline solutions (AS) with different ratios on the development of compressive and flexural strength of RFAC beams in which the most significant factor will be identified for improvement of nonlinear behavior of RC beams through FEM using ANSYS. Objectives of the study are as follows:

- To evaluate the optimal strength of the concrete mixture with the inclusion of FA through the validation of laboratory specimens and numerical models.
- To evaluate the mechanical properties of concrete when different amounts of FA are added to the concrete mixture.
- To evaluate the flexural and nonlinear performance of RFAC beams with different conditions through the virtual lab (FE software).

6.2. Materials and experimental testing

In the experiment, two types of FA are commonly used as source material of concrete in laboratory testing including:

- Class C fly ash where sub-bituminous coals or lignite are used in the production of this type.
- Class F fly ash is known as low calcium fly ash obtained from bituminous coals.

In this research, low-calcium FA known as 450-N (fineness category N, loss on ignition Category B) based on BS EN 450-1 [27], was used. This FA type is widely employed in the UK

which can increasingly be found as the substantial ingredients in the low-carbon blended with PC such as T2PC.

As regards other main ingredients in concrete, coarse aggregate (CAg) (20 mm and 10 mm) and fine aggregate (FAg) were used in the mix design in accordance with BS 1881 [28]. The percentage of aggregates incorporating in the concrete mix design proposed in this study was 43%, 22% and 35%, respectively. Further details subjected to the chemical combination of FA and the mix proportion of this investigation are exhibited in Tables 5 and 6.

Table 5. Requirements for fly ash (EN 450-1, 2012).

Property	Unit	Requirement based on EN 450-1:2012
Loss on ignition for category B	% By mass	2.0–7.0
Water requirement	%	≤95
Fineness fraction for category N ≥ 45 μm	% By mass	≤40
Soluble phosphate (P_2O_5)	% By mass	≤100
Total phosphate	mg/kg	-
Initial setting	Min	2
Sum SiO_2 + Al_2O_3 + Fe_2O_3	% By mass	≥70
Reactive SiO_2	% By mass	≥25
Reactive CaO	% By mass	≤10
Sulphate (SO_3)	% By mass	≤3
Free calcium oxide	% By mass	2.5
Soundness	Mm	≤10
Magnesium oxide (MgO)	% By mass	≤4.0
Chloride (Cl ion)	% By mass	≤0.10

Table 6. Mixture proportion of experimental concrete.

Mix		CAg (kg)		FAg	FA	T2PC	Water	Superplasticizer	w/c
		20 mm	10 mm	(kg)	(kg) (%)	(kg)	(L)	(mL) (2.5%)	
1	PF1000	32.84	16.4	26.52	0 (0%)	12	7.2	0	0.6
2	PF9010	32.84	16.4	26.52	1.2 (10%)	10.8	6.6	30	0.55
3	PF8020	32.84	16.4	26.52	2.4 (20%)	9.6	6	30	0.5
4	PF7030	32.84	16.4	26.52	3.6 (30%)	8.4	6	30	0.5
7	PF5050	32.84	16.4	26.52	6 (50%)	6	6	30	0.5
9	PF3070	32.84	16.4	26.52	8.4 (70%)	3.6	5.7	30	0.48

6.3. Specimen preparation and concrete manufacturing process

Generally, the manufacturing process can be classified into three main steps.

Step 1: All solid materials were mixed approximately 3 min after quantifying by concrete mixer.

Step 2: The alkaline solutions previously prepared in 24 h, prior to blending materials, were poured over the solid materials for those concrete mixes in which the effectiveness of AS is experimentally investigated.

Step 3: Initially, the workability was immediately measured through the slump test before casting fresh concrete. Next, the produced concrete was poured into the cube moulds with the standard

dimension of 150 mm × 150 mm × 150 mm and to reduce the voids of concrete by compacting action on the vibrating table around 1–2 min in accordance with BS 1881 [28]. Then, these specimens were kept at the usual temperature (room heat) between 14–17 °C for 4–5 h. Eventually, the specimens were put in the water bath at the temperature of 21 °C till commencing the compressive tests at the age of 7, and 28 d in this study.

6.4. Validation of compressive strength in experimental and numerical modelling

As mentioned above, material properties and curing conditions are two significant factors for controlling the nonlinear behavior of concrete during applied loading. The results of compressive strength were obtained from the average values of three cube specimens tested for each mixture at the ages of 7, 28 d as shown in Table 7. Also, the workability property through a slump test was conducted on the fresh concrete mixtures in this study.

Table 7. Compressive strength of various mixes without AS.

Mix	%FA	Compressive strength (MPa)		Curing conditions
		7 d	28 d	
PF10000	0	21.56	31.93	Water Bath at 21 °C
PF9010	10	24.99	36.63	Water Bath at 21 °C
PF8020	20	25.24	37.84	Water Bath at 21 °C
PF7030C	30	18.44	31.03	Water Bath at 21 °C
PF5050A	50	11.68	24.53	Water Bath at 21 °C
PF3070A	70	5.49	12.33	Water Bath at 21 °C

RFAC beam specimen with the same size (2400 mm × 250 mm × 150 mm) previously used in section Numerical Calibration with Karnati [13] (Case 1) is considered for this stage as well. Initially, the finite element analysis involves modelling of concrete cubes containing 20% FA and 80% T2PC as the highest value of concrete compressive strength (37.84 MPa) at 28 d (Table 7). Also, the same dimensions (150 mm × 150 mm × 150 mm) and concrete properties experimentally tested in the concrete laboratory is simulated in ANSYS APDL 18.2. This cube is defined in the FE platform (ANSYS) with two points (0, 0, and 0) and (150, 150, 150). For the comprehensive simulation of cube specimen, the top steel plate has been modelled with a thickness of 20 mm due to two following reasons:

Firstly, the simulation of the concrete cubic model in FE software should be similar to its counterpart under laboratory tests. So, it can be seen that the steel plate is actually located on the top surface of concrete specimens over the compressive strength test. Secondly, creating the steel plate on the concrete cube in the modelling process, the stress distribution on the concrete surface is uniformly applied to prevent the top edges of the concrete cube from further displacements leading to more damages due to crushing in these zones and subsequently, the process of analysis will be stopped at this moment. The mesh size of the steel plate is considered the same compared to the cube as shown in Figure 4. The values of main parameters corresponding to nonlinear behavior of concrete based on William-Warenke criteria discussed in section materials constitutive model in FEM are presented in Table 8 and Figure 5.

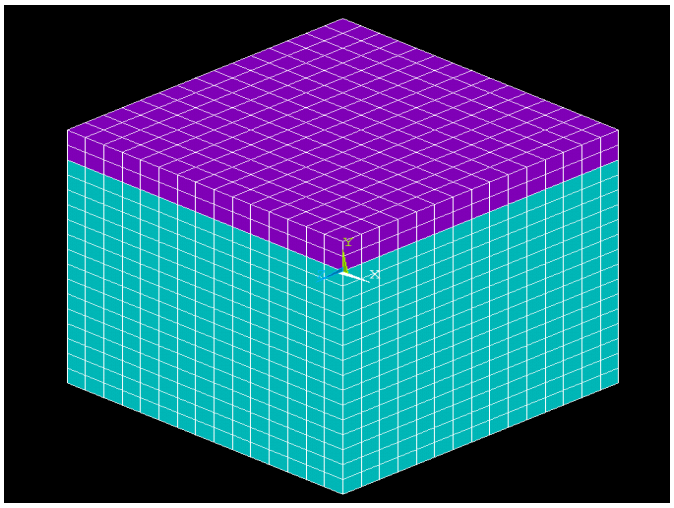

Figure 4. Optimal mesh size (10 mm × 10 mm × 10 mm).

Table 8. Material properties for nonlinear concrete in ANSYS based on the formulas in section materials constitutive model in FEM.

Parameters	Values
The shear transfer coefficient for open cracks (βt)	0.2
The shear transfer coefficient for closed cracks (β_C)	0.8
Uniaxial cracking stress (fr)	46.13
Uniaxial crashing stress ($f'c$)	37.84
Biaxial compressive strength (fcb')	45.408
Ambient hydrostatic stress (σh)	65.46
Hydrostatic biaxial crush stress ($f1$)	54.86
Hydrostatic uniaxial crash stress ($f2$)	65.08
Elasticity modules (E)	22000

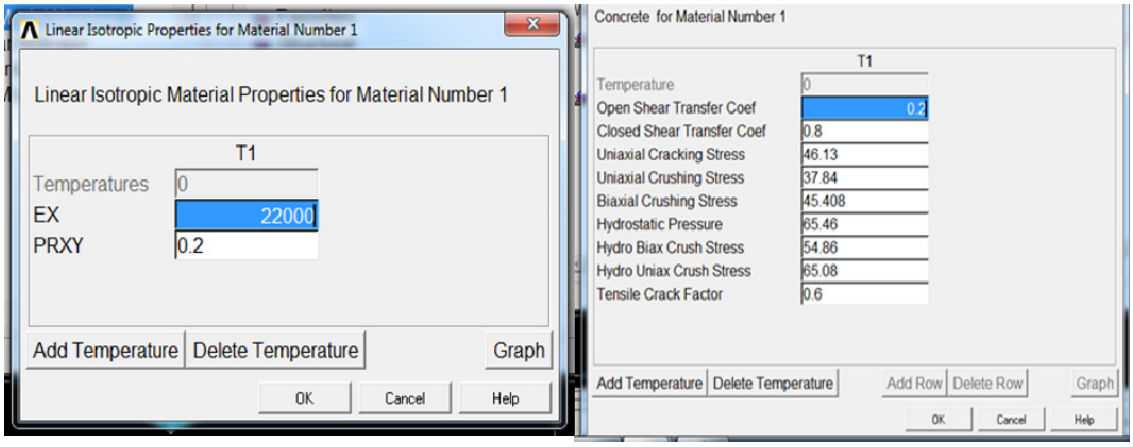

Figure 5. Material models defined for linear and nonlinear behavior of concrete in ANSYS (William-Warenke criteria).

6.4.1. Optimal mesh

Adequate mesh size is the significant factor facilitating analysis of the FE model within a convenient time. In this numerical method, meshing is performed with three different sizes. The coarse size is the mesh with each cube edge divided into six elements. Therefore, the total number of elements is 216 with dimensions of 25 mm × 25 mm × 25 mm. In the second case, each edge is separated into 15 elements which are 3375 elements with the size of 10 mm × 10 mm × 10 mm. Additionally, the finer mesh is also employed with each cube edge distributed into 25 segments consisting of 15625 elements. Eventually, the responses of these models are compared. The second mesh (10 mm) provides satisfactory results; hence the analysis with this mesh size which does not need much computational time is more acceptable compared to other sizes expressed above.

An eight-node brick element SOLID65 is used to model the GPC concrete in the ANSYS FE platform. SOLID65 is used for the 3D modelling of solids with or without reinforcing bars (rebar). The solid is capable of cracking in tension and being crushed in compression which is similar to concrete. The element (SOLID65) is defined by eight nodes having three degrees of freedom at each node: translations in the nodal x, y and z directions. For modelling steel plate, a solid 185 brick element with 8 nodes has been considered in this study. The material property of the steel plate is defined based on linear behavior in which the elasticity modulus and poison ratio are assumed 200 GPa and 0.3, respectively.

6.4.2. Results and discussions

A William-Warenke constitutive model is employed for modelling of nonlinear (cracking and crushing) behavior of a concrete cube. This cube has been tested in the lab with specified conditions. William-Warenke model has nine modelling parameters where these parameters may be changed to calibrate the model.

Three key parameters play a more important role in calibrating the constitutive model. These parameters are ultimate stress, ultimate strain and the slope of the stress-strain curve for the initial part ascending zone of the stress-strain curve. Constitutive model parameters have been selected considering the highest degree of adaption between these three parameters. The ultimate load, stress and strain predicted by the numerical model are 0.52%, 0.47% and 2.66% higher than those achieved in experimental tests (Table 9). Hence, the calibrated model can be used for modelling other structures which are constructed using this material. Achieved stress-strain curves from the constitutive model and experiment are compared in Figure 6. An excellent agreement can be observed in this comparison.

Table 9. Comparison between experimental and theoretical results for numerical simulation (Case 3).

GPC concrete cube	Ultimate load (kN)	Compressive strength (MPa)	Strain at peak stress
EXP	851.4	37.84	0.002069
ANSYS	856.35	38.06	0.001662

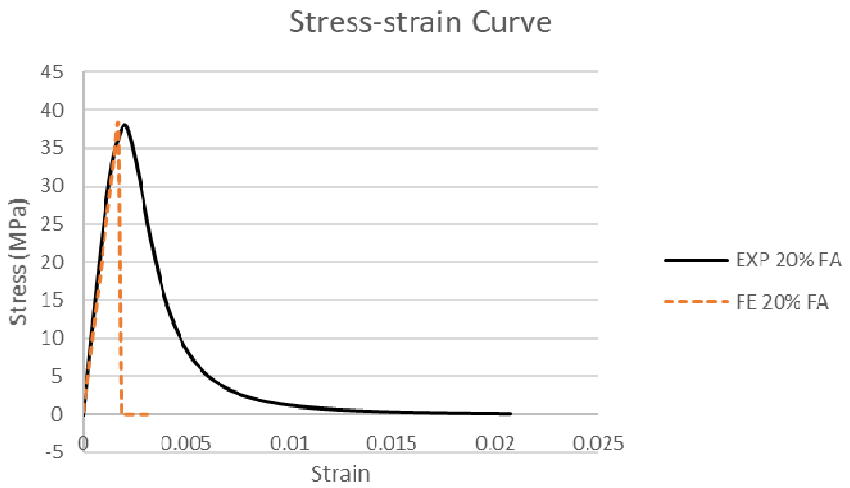

Figure 6. Stress-strain curve for concrete cube with 20% FA in FE and experimental test.

6.5. Flexural strength

In this part, the flexural strength of RAFC beams is evaluated through FEM in ANSYS 18.2 as the validation of concrete properties for both experimental and numerical specimens were previously carried out in sections Numerical Calibration with Karnati [13] (Case 1) and Numerical Calibration with Lisantono et al. [8] (Case 2). The RAFC beam with the same dimensions and mesh size, numerically used by ANSYS in past sections, is selected for this stage as well. Hinge and roller support conditions are considered in the FE model.

6.5.1. Results and discussions

Numerical simulation is used for exploring the efficiency of FA as a PC replacement and AS as well as curing conditions on the flexural strength and nonlinear behavior of RC beams. For RFAC beam with the optimum amount of 20% FA, the maximum applied load is 108.93 kN corresponding to the mid-span displacement of 29.35 mm, whereas the flexural performance of the models containing 10% and 30% FA are found to carry the ultimate loads of 98 kN and 87 kN which are higher than that of the RC beam as the benchmark with 0% FA (Figure 7). This factor can be justifiable due to the reduction of compressive strength of concrete mixtures including FA higher than 20% without using AS given that compressive strength is directly in relation to 6 out of 9 parameters previously discussed in section materials constitutive model in FEM.

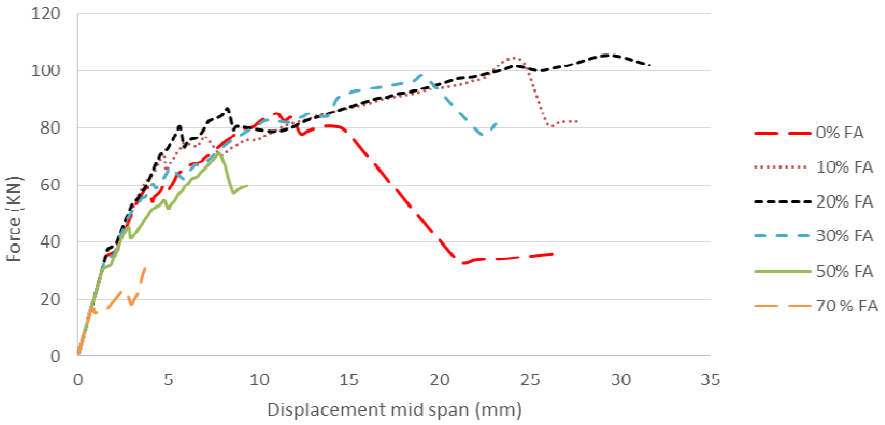

Figure 7. Load vs mid-span deflection for various mixes without AS in FE.

Regarding the plots of load-mid span deflection for RFAC beams with the concurrent use of FA by 30%, 50%, 70% with/without AS (Sodium Sulfate (SS), Sodium Hydroxide (SH)) (see Tables 10 and 11), the cubic compressive strength of these RFAC beams have been previously evaluated in the concrete laboratory. It is evident that the optimum ultimate load-carrying yield capacity of specimens belongs to the RC beam model containing 30% FA without AS. This value (98 kN) is approximately 2 times greater than that of the RC beam with 50% FA and AS as the second-highest optimum load (60 kN) among other RFAC beam models numerically explored in this stage (Figure 8). However, the compressive strength results experimentally obtained for the range of 30–70% FA for the concrete mixes with/without AS reflect a sharp reduction for the compressive strength which is associated with 6 major parameters expressed in section materials constitutive model in FEM and section materials and experimental testing.

Table 10. Concrete mixtures with different ratios of AS for dosages of 30%, 50%, 70% FA.

Mix	% FA	NaOH (gr)	Na_2SiO_3 (gr)	Water (mL)	Na_2SiO_3/NaOH	NaOH molarity (M)	AS/FA
PF7030A	30	250	625	1500	2.5	4.16	0.25
PF7030B	30	250	625	1500	2.5	4.16	0.25
PF5050B	50	428	1070	1500	2.5	7.13	0.25
PF3070B	70	600	1500	1500	2.5	10	0.25

Table 11. Compressive strength of various mixes with AS for the percentages of 30%, 50%, 70% FA.

Mix	% T2PC	% FA	Average compressive strength (MPa)		Curing condition
			7 d	28 d	
PF7030B	70	30	8.14	14.58	Water bath at 21 °C
PF5050B	50	50	5.97	10.55	Water bath at 21 °C
PF3070B	30	70	10.02	15.63	Water bath at 21 °C

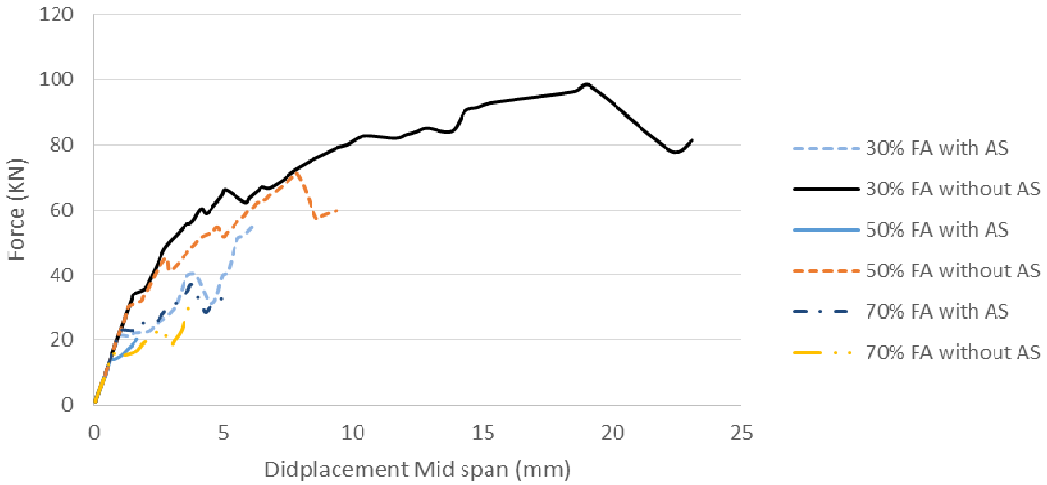

Figure 8. Comparison of flexural strength for mixes with/without AS in FE.

As shown in Figure 9, RFAC beam including 30% FA and AS kept under the heat of oven 110 °C (see Table 12) has the lowest value of ultimate load (25 kN) and relatively low mid-span deflection (2 mm) among all RC beam models. Thus, the typical curing condition (21 °C) based on BS 1881 is strongly recommended in terms of concrete properties such as compressive strength and flexural strength for concrete mixtures with T2PC and low-calcium FA up to 30% as a PC replacement and beyond that, further considerations such as such as the appropriate ratio of alkaline solution and using superplasticizer (SP) such as Glenium 51 in which their chemical combinations are compatible with polymeric products are suggested for this purpose [29–31].

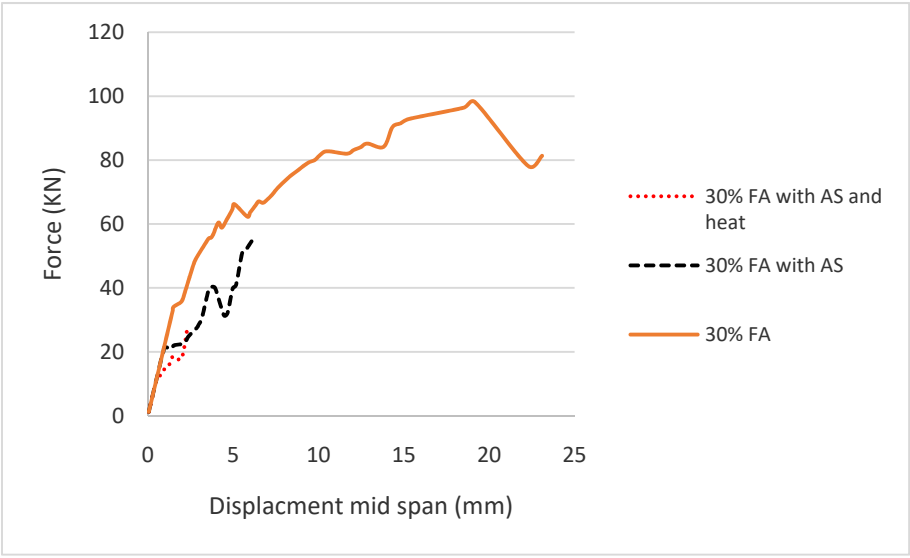

Figure 9. Comparison of flexural strength of RFAC with 30% and different curing conditions in FE.

Table 12. Mix proportion, curing condition and compressive strength of concrete cubes with 30% FA.

Mix	% FA	Compressive strength (MPa)		AS/FA ratio	Curing condition
		7 d	28 d		
PF7030C	30	18.44	31.03	0	Water bath at 21 °C
PF7030A	30	8.28	10.43	0.25	• 24 h heat (110 °C) • 4–5 h keep at room temperature • Water bath at 21 °C
PF7030B	30	8.14	14.58	0.25	Water bath at 21 °C

It is essential to point out that small inclined flexural-shear cracks can be observed while increasing load resulting in large deformation prior to beam collapse. The first crack is to have appeared in the maximum moment region and subsequently, this trend is followed by additional flexural cracks. Therefore, a large inclined flexural-shear crack appeared between load and support, subsequently, the beam abruptly collapsed. The crack pattern of RFAC beam specimens is virtually simulated through ANSYS 18.2 in this study. The RFAC beam with the highest ultimate load containing 20% FA as the replacement of T2PC is chosen for this purpose (Figure 10a). The first cracking of FEM for this RFAC beam appeared at the load of 21.2 kN due to the exceeding modulus of rapture (3.94 MPa).

The FE results in section Numerical Calibration with Karnati [13] (Case 1) has shown that the first cracking load for RC beam in the experimental study by Chahrour and Soudki [25] and numerical study by Karanti [13], were 21.87 kN and 18.14 kN, respectively (Table 2). So, the comparison of the first cracks in the previous studies and the present study indicates that the numerical results obtained from FEM are in close agreement with each other. Indeed, with the enhancement of the load at each step, the cracks start to appear under applied loads and flexural cracks from mid-span develop to fixed support end (Figure 10b).

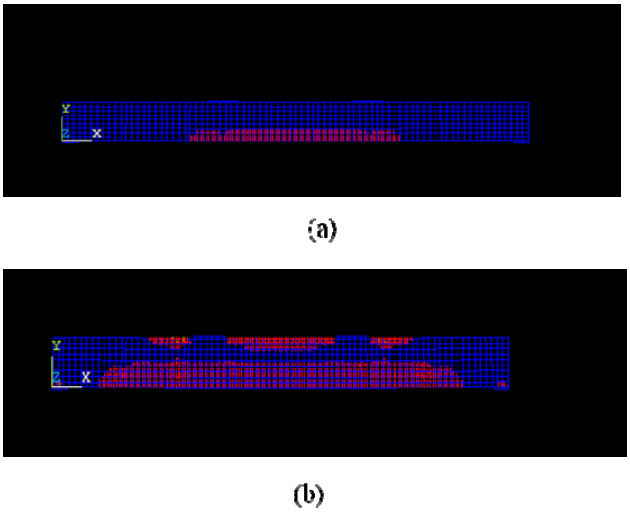

Figure 10. Cracks developed in RFAC beam with 20% FA (a) at load 21.2 kN, (b) at ultimate load (108.93 kN) for numerical solution (Case 3).

7. Conclusions

Based on the achieved experimental and numerical results from this study, the following conclusion can be drawn:

- The compressive strength and flexural strength of low calcium FA based geopolymer concrete are enhanced with the inclusion of FA as T2PC replacement up to 20% at 28 d.
- The flexural strength of RFAC beams containing 30% FA without heat and AS has the highest flexural strength than those with 30% FA, AS and heat. Therefore, the typical curing condition (21 °C) based on BS 1881 is deeply recommended for concrete properties such as compressive strength and flexural strength for concrete mixtures with T2PC and low-calcium FA up to 30%.
- The concurrent usage of FA with a dosage of over 20% along with alkaline solutions significantly decreased the flexural strength of RC and RFAC beams.
- FE models of RFAC and RC beams, simulated in ANSYS 18.2 utilizing the dedicated concrete element (Solid 65) as a smeared crack model, has accurately captured the nonlinear flexural performance of these systems up to collapse.
- The failure mechanism of RFAC and RC beams is modelled quite well by employing FE. Also, the prediction of failure load has very high accuracy compared to that obtained during laboratory testing.
- The numerical methods used in this study for both RC and RFAC beams with the concrete properties from experimental tests have provided a deeper comprehension for future utilization of FE software to evaluate the nonlinear behavior of the concrete beams with the inclusion of FA as the PC replacement.
- According to outputs obtained from FE models, it is proved that the numerical results are highly dependent on mesh size, material properties, load increment, etc.
- The involvement of FA in the concrete mixture has a marginal effect on the stiffness (Ec) of RFAC beams.

Conflict of interest

There is no conflict of interests between authors.

References

1. Ismail AH, Kusbiantoro A, Chin SC, et al. (2020) Pozzolanic reactivity and strength activity index of mortar containing palm oil clinker pretreated with hydrochloric acid. *J Clean Prod* 242: 118565.
2. Tee KF, Mostofizadeh S (2021) A mini review on properties of Portland cement concrete with geopolymer materials as partial or entire replacement. *Infrastructures* 6: 26.
3. Mostofizadeh S, Tee KF (2019) Evaluation of impact of fly ash on the improvement on type II concrete strength. *Proceedings of the 39th Cement and Concrete Science Conference*, 190–193.
4. Gharehbaghi K, Tee KF, Gharehbaghi S (2021) Review of geopolymer concrete: A structural integrity evaluation. *IJFE* (in press).

5. Samad AAA, Mohamad N, Ali AZM, et al. (2017) Trends and development of green concrete made from agricultural and construction waste, *Advanced Concrete Technology and Green Materials*, Johor: Penerbit UTHM.
6. Tee KF, Agba IF, Samad AAA (2019) Experimental and numerical study of green concrete. *Int J Forensic Eng* 4: 238–254.
7. Samad AAA, Hadipramana J, Mohamad N, et al. (2018) Development of green concrete from agricultural and construction waste, In: Sayigh A, T*ransition Towards 100% Renewable Energy*, Springer, Cham, 399–410.
8. Golewski GL (2020) Changes in the fracture toughness under mode II loading of low calcium fly ash (LCFA) concrete depending on ages. *Materials* 13: 5241.
9. Golewski GL, Gil DM (2021) Studies of fracture toughness in concretes containing fly ash and silica fume in the first 28 Days of curing. *Materials* 14: 319.
10. Golewski GL (2021) The beneficial effect of the addition of fly ash on reduction of the size of microcracks in the ITZ of concrete composites under dynamic loading. *Energies* 14: 668.
11. Lisantono A, Wigroho H, Purba R (2017) Shear behavior of high-volume fly ash concrete as replacement of Portland cement in RC beam. *Procedia Eng* 171: 80–87.
12. Annapurna D, Kishore R, Sree MU (2016) Comparative study of experimental and analytical results of geopolymer concrete. *IJCIET* 7: 211–219.
13. Karnati V (2016) Flexural response of reinforced concrete beams using various cementitious materials [Master's Thesis]. University of Toledo.
14. Dahmani L, Khennane A, Kaci S (2010) Crack identification in reinforced concrete beams using ANSYS software. *Strength Mater* 42: 232–240.
15. Vasudevan G, Kothandaraman S, Azhagarsamy S (2013) Study on non-linear flexural behavior of reinforced concrete beams using ANSYS by discrete reinforcement modeling. *Strength Mater* 45: 231–241.
16. Ansys Fluent 14.0: User's guide, 2011. Available from: https://www.scribd.com/doc/140163383/Ansys-Fluent-14-0-Users-Guide.
17. Nguyen K, Ahn N, Le T, et al. (2016) Theoretical and experimental study on mechanical properties and flexural strength of fly ash-geopolymer concrete. *Constr Build Mater* 106: 65–77.
18. Popovics S (1970) A review of stress-strain relationships for concrete. *ACI J* 67: 243–248.
19. Isojeh B, El-Zeghayar M, Vecchio F (2017) Simplified constitutive model for fatigue behavior of concrete in compression. *J Mater Civil Eng* 29: 04017028.
20. Buckhouse ER (1997) External flexural reinforcement of existing reinforced concrete beams using bolted steel channels [Master's Thesis]. Milwaukee: Marquette University.
21. Halahla A (2019) Identification of crack in reinforced concrete beam subjected to static load using non-linear finite element analysis. *CEJ* 5: 1631–1646.
22. Kachlakev D, Miller TR, Yim S, et al. (2001) Finite element modeling of concrete structures strengthened with FRP laminates. FHWA-OR-RD-01-17, Oregon Department of Transportation Research Section
23. Desai YM, Mufti AA, Tadros G (2002) User manual for FEM PUNCH, Version 2.0. ISIS Canada.
24. Dawari V, Vesmawala G (2013) Modal curvature and modal flexibility methods for honeycomb damage identification in reinforced concrete beams. *Procedia Eng* 51: 119–124.

25. Chahrour A, Soudki K (2005) Flexural response of reinforced concrete beams strengthened with end-anchored partially bonded carbon fiber-reinforced polymer strips. *J Compos Constr* 9: 170–177.
26. Ramazanianpour A, Malhotra V (1995) Effect of curing on the compressive strength, resistance to Chloride-ion penetration and porosity of concrete incorporating slag, fly ash or silica fume. *Cement Concrete Comp* 17: 125–133.
27. British Standards (1983) Testing concrete—Part 116: method for determination of compressive strength of concrete cube, BS 1881-116. Available from: https://989me.vn/en/download/Other-Items/BS-1881-116-1983-Testing-concrete-Part-116-Method-for-determination-of-compressive-strength-of-concrete-cubes.html.
28. Getahun MA, Shitote SA, Gariy ZCA (2018) Experimental investigation on engineering properties of concrete incorporating reclaimed asphalt pavement and rice husk ash. *Buildings* 8: 115.
29. Xie J, Kayali O (2016) Effect of superplasticizer on workability enhancement of class F and class C fly ash-based geopolymers. *Constr Build Mater* 122: 36–42.
30. Nematollahi B, Sanjayan J (2014) Effect of different superplasticizers and activator combinations on workability and strength of fly ash based geopolymer. *Mater Design* 57: 667–672.
31. Alrefaei Y, Wang Y, Dai J (2019) The effectiveness of different superplasticizers in ambient cured one-part alkali activated pastes. *Cement Concrete Compos* 97: 166–174.

AIMS Press